



Karst geology and mitigation measures for hazards during metro system construction in Wuhan, China

Xiuling Wang¹ · Jinxing Lai¹ · Siyue He¹ · Rodney Sheldon Garnes² · Yuwei Zhang³

Received: 22 October 2018 / Accepted: 6 June 2020 / Published online: 15 June 2020
© Springer Nature B.V. 2020

Abstract

Karst geology is widely distributed in China; the great differences in natural conditions bring it an array of characteristics in different regions. There is a huge area of the buried karst in Wuhan, exhibiting a unique, but complicated engineering geological environment. This paper summarizes the geological conditions in Wuhan, with special focus on its karst geology. At present, a total of six karst belts have been detected, and they were divided into five structure types. For shield tunnelling in karst region, some problems such as water ingress or mud inrush, partial ground collapse, damage or failure of shield machine, and metro operation and management issues may be raised as a result of the activity of the karst geology. To prevent occurrence of possible hazards, a series of countermeasures suggested for hazard and risk mitigation were discussed in this paper. A case history, where the study section belongs to the Wuhan metro line 6, is referred to evaluate effectiveness of the adopted treatment measures. The feedbacks demonstrated that water ingress was successfully avoided, and ground deformation was effectively controlled in the study section throughout the construction phase. This study can provide significant reference information and experience for metro tunnel constructed in karst region.

Keywords Karst geology · Metro tunnel · Geologic hazards · Prevent and countermeasures · Case history

1 Introduction

Because of the largest karst distribution area, China is home to some of the rarest types of karst in the world (Huang and Cai 2007; Wang et al. 2004). It is mainly developed in carbonate region, with an area of about 1.3 million square kilometres, accounting for about

✉ Jinxing Lai
lajinxing@chd.edu.cn

¹ School of Highway, Chang'an University, Middle of South 2nd Ring Road, Xi'an 710064, Shaan'xi Province, China

² School of Graduate Studies, University of the West Indies, Cave Hill Campus, Cave Hill, St. Michael, Barbados

³ School of Civil Engineering, Xi'an University of Architecture and Technology, Xi'an 710055, China

13.5% of total land area of China (Wang et al. 2020a). Owing to complexity of control factors and diversity of developmental morphology in karst, it brings a series of difficulties to design and construction in civil engineering (Zini et al. 2015; Song et al. 2020, Liu et al. 2020a, b). A large number of the hazards and incidents caused by adverse impacts of the karst have been recorded when a tunnel passes through the karst region (Alija et al. 2013; Qiu et al. 2020a; Cheng et al. 2020). Thus, to minimize the risk of the geological hazards, many scientific findings are available regarding the aspects of the karst formation mechanism, development regularity, and their impacts on metro systems. Based on the numerical and analytic methods, Wang et al. (2018c) studied influence of karst cave span, height–span ratio, and filling degree on safe thickness of cave roof, and then proposed a predictive model for the safe thickness of cave roof. In order to deal with possible hazards during shield tunnelling undergoing karst caves, Cui et al. (2015) developed a construction framework consisting of field investigation, judgment, treatment, and effectiveness check, to avoid the occurrence of excessive ground surface settlement. Sun et al. (2018) analysed development conditions, mechanism, and mode with reference to the karst in Jinan, and proposed the method of “shallow-deep” and “region-target” for use in karst detection. Despite all this, it is noted that the vast karst geology still seriously affects the development of Chinese transportation infrastructures (Li et al. 2018; Zhang et al. 2020a, b).

Wuhan, one of the oldest megacities in China, is located in the Jiangnan Plain and administrates seven main urban districts (main urban area) and six distant urban districts (distant urban area), as shown in Fig. 1. The karst deposited in limestone strata is mainly developed in its main urban area. (WGSC 2018). Dramatically, the overall city’s area is 8494 km², with a limestone area of 1100 km², which provides necessary materials for karst development. The presence of karst often leads to striking hazards during the rapid urbanization. Over the recent twenty years, more than twenty hazards caused by karst activity have occurred in Wuchang, Hongshan, Hanyang and Jiangxia districts (Zhou et al. 2017; Fan 2006). The karst-associated hazards not only affect project construction, but also cause huge economic losses. Wuhan has experienced intensifying

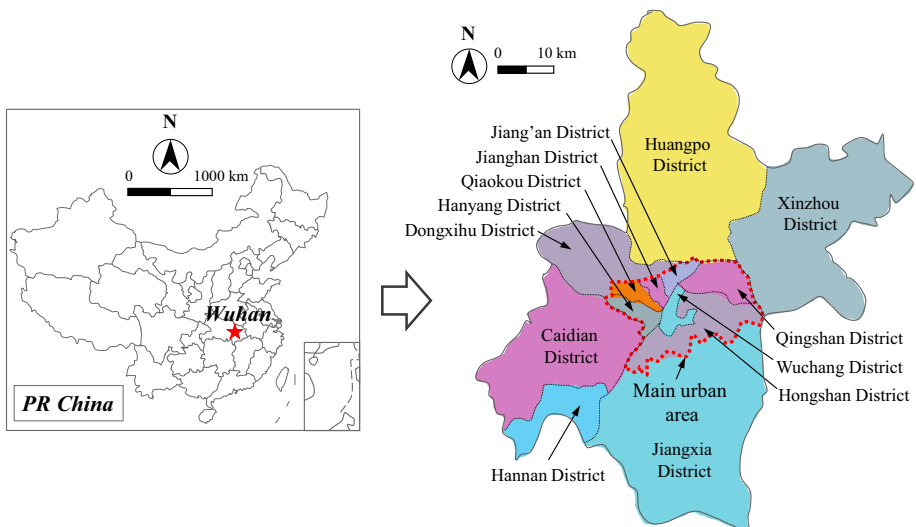


Fig. 1 Location of Wuhan and its administration district division

demands for urban expansion; its infrastructure construction has come into a boom in recent years (Bai et al. 2016; Wang et al. 2020b, c, d). The metro system’s efficiencies are marked by saving land and energy, reducing noise and pollution, which makes it the best choice for modern cities to develop urban transportation. Also, shield-based excavation plays an indispensable role in metro tunnel construction (Maeda and Kushiyama 2005; Zhang et al. 2020c). Fig. 2 presents the UMT Network Planning in Wuhan city, where a 439.1 km urban rail transit network system will be established by 2020 (WHRT 2018). However, the complex geological conditions in Wuhan bring difficulties and challenges to metro tunnel construction in terms of some metro systems passing through karst regions. A series of geo-hazards have been confirmed from the past engineering research data and experiences. Karst strata with water-rich caves or poor load-bearing capacity may cause water ingress, mud inrush, formation sliding, tunnel structure damage, or even ground collapse, etc. (Ma et al. 2020, Qin et al. 2020, Wang et al. 2018a, b). The previous investigations were mainly conducted based on the specific engineering events. Thus, it is still an increasing demand for studies on how to construct and extend the operational life span of metro system constructed in karst regions (Li et al. 2015; Knez et al. 2008; Wang et al. 2016a; Wu et al. 2020c; Yang and Xiao 2016; Cao et al. 2020).

In view of the lack of a systematic summary on karst geology and protective measures on hazards during metro system construction in Wuhan, this paper pays more attention to: (1) present a brief introduction to features, distribution and structures of karst geology in Wuhan, (2) to discuss possible hazards and damages for shield tunnelling in karst regions, and (3) to introduce some countermeasures for hazards mitigation and treatment effectiveness on basis of a case history.

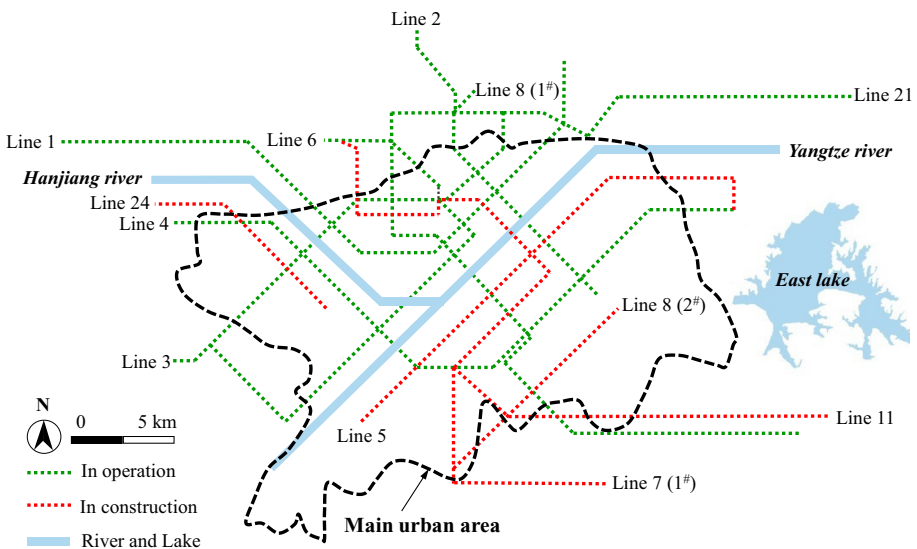


Fig. 2 Planning map of the Wuhan metro system by 2020

2 Geological and hydrogeological conditions in Wuhan

The overall landform in Wuhan is mainly dominated by typical hilly plain, and the lithology is mainly composed of bedrock and loosening overlay. The overall geomorphology of the city is transformed from an erosion-accumulation area to an alluvia-diluvia area (i.e., from Grade-III terrace to Grade-I terrace of the Yangtze river, in which the stepped topography stretches along the river valley due to the erosion and accumulation), with an elevation varying from 21.6 to 26.8 m. The typical geological section of the plain area in Wuhan is shown in Fig. 3.

There are two modes of the rock-soil structures in the main urban area. One of these two modes is the Grade-I terrace region, where the upper part distributes soft clay and sandy soil of the Holocene series. This region has a typical dualistic structure of the upper soft soils and lower sand, with an overburden thickness varying from 30 to 60 m. The other one is the Grade-II to III terraces region, in which the upper part distributes plastic clay and gravel soil of the mid-upper Pleistocene, with an overburden thickness varying from 12 to 30 m. The underlying bedrock of Silurian Cretaceous system can be divided into soluble carbonatite and insoluble clasolite. The soluble carbonatite is distributed in the core and two limbs of the regional syncline. The soluble rocks of the syncline core region are developed in Daye formation of the lower Triassic, and some of them are in the Guanyinshan and Lushuihe formations. The carbonatite in the two limbs is developed in the Huanglong and Chuanshan formations of the upper Carboniferous, and the Qixia formation of the lower Permian. They are separated by insoluble clasolite that developed in the Gufeng formation of the Permian. Figure 4 shows the geology map of Wuhan.

Wuhan has a huge area of the surface water body due to its low-lying topography. The strata are commonly developed with karst caves in different properties as a result of the wide distribution of karst geology. The groundwater is generally stored in these caves that marked by sharp variations in the quantity and size. It mainly consists of the perched water in loosely backfill layer, the Quaternary pore confined water in sandy soil layer, the fracture karst water in carbonatite, and a small amount of the fracture water in clasolite layer, as indicated in Table 1. The Quaternary pore confined water and carbonate fracture karst water along the river shows a complementary relationship with the Yangtze river water. At the same time, the amount of the fracture karst water in buried carbonate layers is controlled by the lithology, fracture structure and development degree of karst, etc.

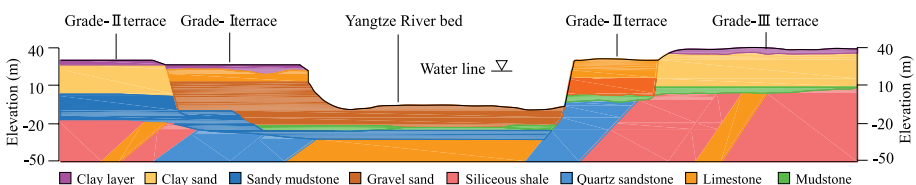


Fig. 3 Geological profile of plain area in Wuhan. After Gao (2017)

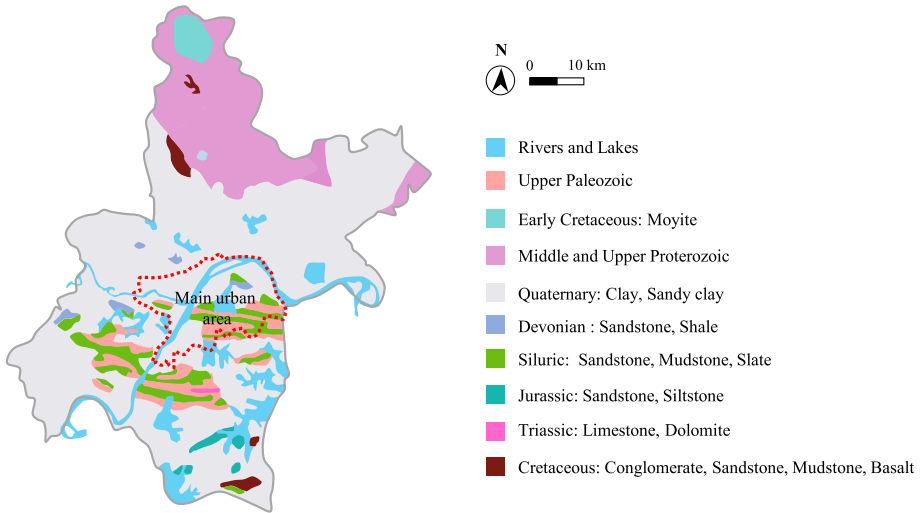


Fig. 4 Geological map of Wuhan

3 Karst geology in Wuhan

3.1 Features and distribution

Wuhan situates at the north margin of the Yangtze paraplatform and the southern margin of the Qinling folding system. The metamorphic rock series of the Archean and Proterozoic are mainly developed in the Qinling folding system, but the carbonate rock series are missing. The Yangtze paraplatform region, during the period from the middle Silurian to the middle Triassic, was in a depositional environment of shallow sea and open platform. After the twice transgression-regression cycles, forming the Huanglong formation of the middle Carboniferous, the Qixia formation of the lower Permian, and the Daye and Guanyinshan formations of the lower Triassic, which is advantageous to development and evolution of the karst in Wuhan.

As a result of the long-term tectonic actions, the underlying bedrock approximately runs from east to west, as indicated in Fig. 5. Based on the topographical relationship between the limestone depositional districts and the Yangtze river, there are six karst belts from north to south were detected in the main urban area and its adjacent areas, which spread across the Yangtze river in east–west direction (Luo 2013). Table 2 presents the characterization of these karst belts.

KB1: The Tianxingzhou karst belt is mainly composed of the carbonate rocks of the Yushan-Qingshan syncline, and the core and two limbs of the Jinggangshan syncline.

KB2: The Daqiao karst belt is located near the reverse Daqiao syncline where the core is the Daye formation of the Triassic, and the two limbs is the Permian strata.

KB3: The Baishazhou karst belt belongs to the Xinglong-Baozixie compound reverse syncline, and mainly consists of limestone of the Xinglong-Baozixie reverse syncline core of the Daye formation, and the two limbs of the Huanglong and Qixia formations.

KB4: The Zhuankou karst belt mainly consists of the carbonate belonging to the core and two limbs of the Zhuankou-Liufangling compound syncline.

Table 1 Distributions and description of the groundwater in Wuhan. Data from Ning et al. (2006)

Groundwater types	Soil compositions	Thickness (m)	Depth (m)	Permeability (m/d)	Influence radius (m)
Perched water	Silt, silty clay, gravel and fine sand	3.2–44.9	0.05–5	0.26–87.08	81.2–466.6
Pore confined water	Gravel, grit stone and medium sand	1.6–33.2	8–26	4.2–47.24	44.6–508
Fracture karst water	Carbonatite	221.8–281	–	0.15–3.09	–
Fracture water	Silicolite, conglomerate and sandstone	–	–	0.72	–

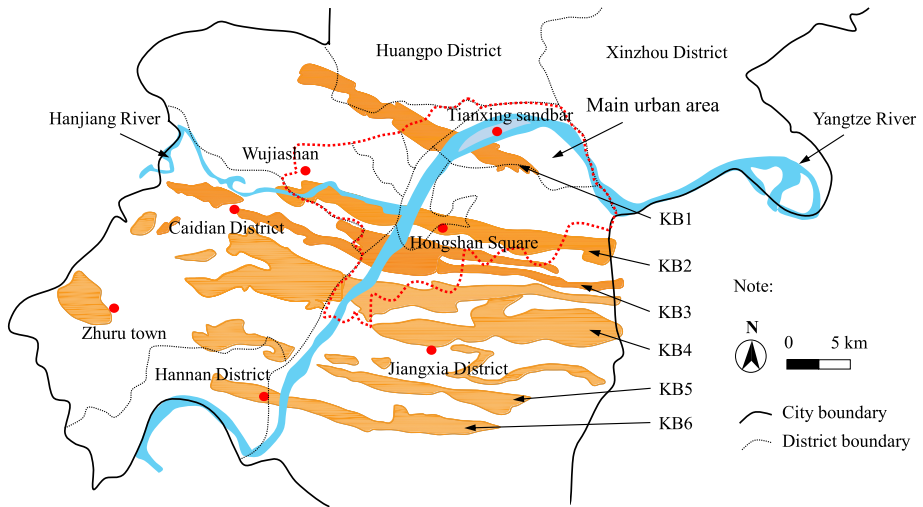


Fig. 5 Distribution of the karst belts in Wuhan. After Luo (2013)

Table 2 Summary of karst belts in Wuhan. Data from Luo (2013)

No.	Name	Length (km)	Width (km)	Area (km ²)	Affected metro line
KB1	Tianxingzhou	39	1.6–3.6	96.8	Line 3
KB2	Daqiao	47	0.5–2.4	105.7	Lines 2, 3, 4 and 6
KB3	Baishaozhou	63	1.1–6.2	150	Lines 2, 3, 6 and 11
KB4	Zhuankou	56	3.2–15	541.3	Lines 2 and 6
KB5	Junshan	39	0.9–3.9	166.2	Lines 4 and 5
KB6	Hannan	35	1.5–1.9	7.8	Lines 5 and 7

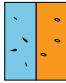
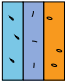
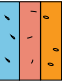
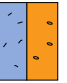

KB5: The Junshan karst belt was formed in carbonate from the Junshan-Tianliangshan syncline, and the core and two limbs of the Yuanlongshan-Guanjiafan syncline.

KB6: The Hannan karst belt is located in the core of the Doubucun syncline and is of north-west extended.

3.2 Structure classification

The development degree of the buried karst weakens with the increase in its buried depth. There are many karst types, but in Wuhan they are mainly in caves, dissolved holes and karst fissures. The carbonatite is usually covered with rock, old clay and silty sand. As shown in Table 3, karst geology in Wuhan could be classified into five structural types based on the differences in the overlying strata and engineering performance of rock-soil layers. The diverse karst structures may produce geological hazards under the influence of different disaster factors.

Table 3 Structure classification for karst geology in Wuhan. After Luo (2013)

Type	View example	Description	Characteristics
I		Carbonate is directly covered with sandy soil	Sandy soil directly leaks through gaps and holes, causing ground collapse and leading to geological hazards
II		There is a Pleistocene clay with a thickness of less than 3 m between sandy soil and limestone	Due to the long-term and groundwater actions, there may be soil holes in old clay soil layer above the limestone. The collapse may arise if the continuity of old clay soil is failure
III		A red Jurassic or Cretaceous-Paleogene bed exists between sandy soil and limestone	Damage to the red beds may cause ground collapse, for example, the opening drilling hole is connected to the sandy soil
IV		Carbonate rock is directly covered with cohesive soil	As a result of the long-term and groundwater actions, there may be soil holes in the old clay soil, and if the soil cavities further develop, and the strata may collapse
V		Limestone is directly covered with red bed	Its structure is stable, and there is a small occurrence probability of karst geological hazards

4 Hazards and damages in metro system

Previous engineering experiences confirmed that karst caves result in many hazards in engineering construction, and the following problems may be encountered during Wuhan metro construction in karst region: (1) water ingress and mud inrush, (2) partial karst ground collapse, (3) damage and failure of shield machine, and (4) metro operation and management issues.

4.1 Water ingress and mud inrush

Karst caves were formed by a long-term dissolution of the groundwater (Waltham and Fookes 2003). The metro tunnels in Wuhan often pass through the water-rich stratum with karst caves. The adverse impacts from karst water on fractured rocks not only reflect in its softening effect, but also the corrosion action, resulting in appearance of water-ingress structural planes and reduction in rock strength (Gui et al. 2017; Qiu et al. 2020b). Some adverse aspects such as the accumulation of groundwater, rapid decline in karst-water level, and fast flowing of groundwater in karst systems may create negative pressure in fissures near bedrock surface. To reach a new pressure balance, pore water in overlying soil layers would be accelerated to replenishment karst aquifer, which will increase the hydraulic gradient acted on soft rocks and soils near the concentrated seepage area. The insufficient roof thickness of karst caves cannot bear karst water pressure duo to metro tunnelling exposing the caves or excavation of upper rock and soil layers, and then the cave roof could be breakdown, causing water ingress and mud inrush (Fig. 6).

4.2 Partial karst ground collapse

The ground subsidence faced by metro construction can be categorized in the following two forms: karst surface collapse and karst foundation collapse. The karst cave, a kind of underground hole, is formed by karst action in soluble rocks, and it is usually stable and safe when it is in natural state (Wang et al. 2016b; Huang et al. 2017). The tunnelling disturbance during the metro tunnel passing through the karst region where the caves develop,



Fig. 6 Illustration of water ingress and mud inrush in metro system (Ren et al. 2016; Wang 2014)

will lead to a destruction on the natural balance of the caves. It may cause cave roof to fall off and ground settlement exceeding standard value, or even lead to a ground surface or foundation collapse. In addition, dewatering works in metro construction may produce a devastating and irreversible destruction on cave's roofs. The water-level-decline-induced lag effect forms an osmotic pressure, which will further erode and scour the cave roof overlay, and then accelerating the ground destruction. The collapse hazards not only threaten metro project, but also cause damages to nearby buildings and traffic systems around the area (Fig. 7).

4.3 Damage and failure of shield machine

The karst caves have significantly adverse impacts on the shield cutter head, segments and structure stability, whereas the use of shield machines may be dramatically threatened by a variety of karst caves during Wuhan metro construction. Thus, a favourable tunnelling environment is crucial for a shield tunnel constructed in karst region so as to ensure safe excavation. In the construction area, karst water in caves may swarm into shield, resulting in losing control of the machine postures. When shield excavation faces the karst caves below the tunnel, these corrosion-induced caves and their fillings with poor load-bearing capacity always cannot be able to meet safe construction requirements. In this case, the downward postures of shield cutter head may easily lead to the shield jammed in caves or overproof displacements of shield segments. In some extreme situations, the shield machine may have to embrace the risks of side slip, fall, or even subsidence, as a result of the cave roof thickness failing due to an imbalance in upper pressure.

4.4 Metro operation and management issues

The metro system generally services for decades, or even hundreds of years; however, the potential hazards caused by karst caves may threaten the long-term stability of metro tunnel structures. The possible operation and management threats in metro system may come from any of the following aspects: (a) under the influence of groundwater activities and environmental changes, caves filled with poor fillings may be confronted with body collapse as time goes on (Wei and Sun 2017; Wu et al. 2020a, b), (b) post-construction differential settlement of movement joints in karst region, (c) soil layers with certain conditions may enhance a new development of karst caves in the



Fig. 7 Photograph of ground collapse induced by shield tunnelling in (a) Wuhan metro line 3 and (b) metro line 6 (Qu 2017)

region nearby, (d) the adverse impact from train vibration during metro operation on karst caves, (e) potential water-flow-driven sand loss due to the dewatering activity of a foundation pit near the tunnel, and (f) differential settlement between various strata and potential leakage from shield segment.

5 Prevention and treatment of hazards induced by karst

Generally, tunnel line selection in karst area is a rather time-consuming work of the metro construction. To prevent issues that cause cost overruns or delayed project delivery, the tunnel lines should be designed to avoid karst caves or, if they are unavoidable, to extend through the regions with fewer and smaller caves (Cui et al. 2015). When passing through the caves is unavoidable, they need to be treated before tunnelling so as to avoid the safe issues. Usually, the effective treatment measures are used to provide adequate load-bearing capacity, reduce deformation of metro structures, improve strength of the cave fillings, and control differential settlement of movement joints, and so on. Thus, the aforesaid hazards could be prevented by: (1) karst cave detection and early warning, (2) slurry grouting methods, (3) ground improvement, (4) waterproofing techniques, and (5) shield machine parameter optimization.

5.1 Karst cave detection and early warning

Figure 8 presents a framework consisting of cave early detection and early warning system for use when a metro system is constructed in the karst region. An advanced detection system is crucial for the planning and implementing of the construction phase, safety and health of employees, follow-up maintenance and later tunnel construction within the same area. It is considered one of the most efficient way for exploration of unfavourable engineering geology, and then can give an early warning of risk. Several cave detecting techniques have been successfully employed in Wuhan metro system, these mainly includes geological radar, computed tomography (CT), transient electromagnetic method, high-density resistivity method and geological drilling. Usually, the geological radar usually does well in gaining geometric characteristics and filling degree of the karst caves, while the CT is always used to obtain the rock-soil boundary and their fragmentation degree. The high-density resistivity method is commonly adopted to detect the pattern and occurrence features of the stratum section, while the geological drilling is effective in determining the physical and mechanical parameters of karst geology. The reasonable techniques could be employed according to the priorities of the detection purpose during tunnel construction. These methods were also technicality complimented by other survey methods such as pumping test, groundwater quality analysis and petrochemical analysis. The risk assessment in terms of such aspects as cave location, scale, quantity and filling degree should be conducted first to determine whether to implement the treatment or not, or what kind of construction programs can be effectively used.

5.2 Slurry grouting techniques

Figure 9 illustrates an example of grouting filling in karst caves, which usually realized by the order of pre-backfilling and post-grouting. It can significantly overcome malpractices

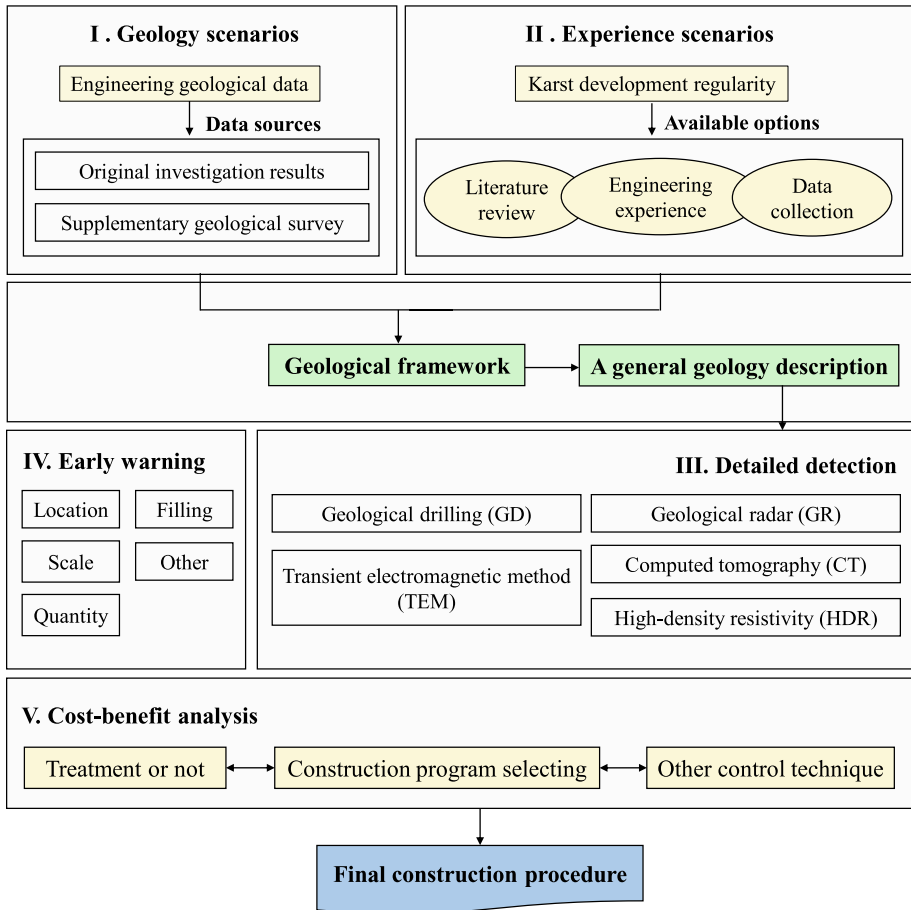
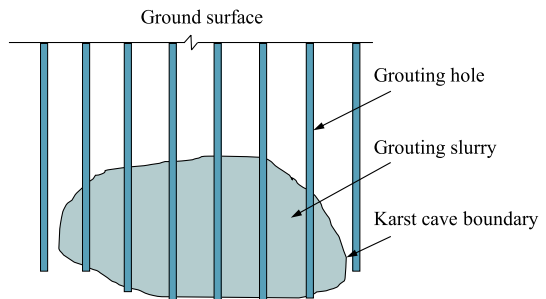


Fig. 8 Illustration of a work framework for metro tunnel construction in karst region

Fig. 9 Illustration of grouting filling. After Cui et al. (2015)



of weak load-bearing capacity of cave fillings and resist the water pressure from water-rich caves during metro tunnelling, and thus reducing the possibility of the water ingress and mud inrush.

Figure 10 shows grouting treatment criteria of karst caves around metro tunnel (TROWM 2014). The karst caves above metro tunnel’s axis must be treated. And if the cave horizontal distance L from the tunnel is less than 3 m, the caves must be treated. Accordingly, if the cave vertical distance D in rock stratum is less than 6 m while that is less than 8 m in soil stratum, then the caves must be treated. If the cave height H is less than 1 m, it can be treated by static pressure grouting (SPG) with pure cement pulp. If the H is between 1 and 3 m, it can be treated by intermittent SPG with a 20-min grouting time and 6-h intermittent time. If the H is between 3 and 6 m, it must be treated with beforehand gravel and followed by slurry grouting. If the L is more than 3 m and the D is more than 8 m, it does not have to be treated. However, if the H is more than 6 m, a special treatment scheme is required.

5.3 Ground improvement

An improvement method for rock cover, shown in Fig. 11, which is similar to the concept of subgrade construction, was developed by Li and Tao (2015) to improve the load-bearing capacity of bedrock and stabilize the ground for safe construction and operation. When metro tunnel passes through the region with karst caves, the full-paved improved-soil treatment can be carried out at the interface between favourable ground and formation developed with karst caves, so as to reinforce natural ground. This method can effectively control uneven settlement of foundation induced by variations of rock and soil properties, and significantly improve load-bearing capacity of the underlying layer, and thus reduce construction risks accordingly.

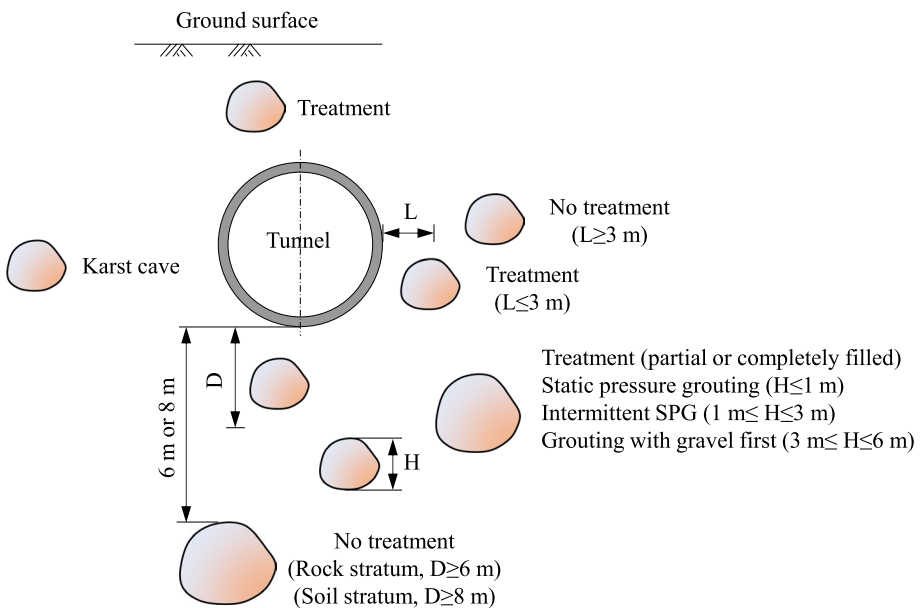


Fig. 10 Treatment criteria of karst caves around metro tunnel. *Note:* L is the cave horizontal distance from the tunnel, D is the cave vertical distance from the tunnel and H is the cave height (Cui et al. 2015; TROWM 2014)

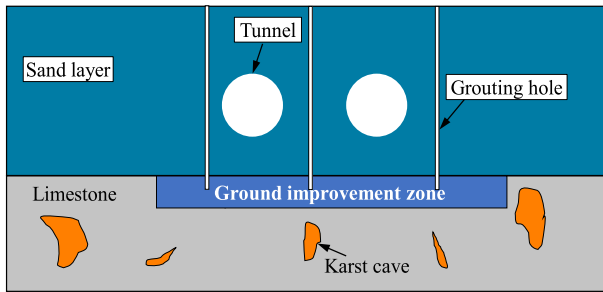


Fig. 11 Illustration of ground improvement. After Li and Tao (2015)

Figure 12 depicts an example of basement reinforcement by jet-grouting pile, and it can be effectively employed for basement treatment of metro stations constructed in area with karst caves. The application of lattice-type jet-grouting pile can significantly slow down the water flow by dividing the basement into multiple regions. This method can also prevent sand loss, improve basement strength, and then reduce occurrence risk of ground collapse as well as other geo-hazards.

5.4 Waterproofing techniques

Apart from the implementation of artificial dewatering measures and the installation of waterproofing elements in tunnel liner structures, the diaphragm wall is always employed in open-cut metro station to remove cave-water-flow-induced hazards, that may affect metro later operation (Fig. 13). It can cut-off hydraulic connection inside and outside enclosure and forms a closed waterproofing system (Ding et al. 2011). Then, it contributes to ground reinforcement and interrupt of water flow so as to realize the seepage prevention and plugging. The advantage of this method is, after necessary treatment for karst caves inside the wall area, the risks of geo-hazards outside the treatment region can be significantly reduced at the same time.

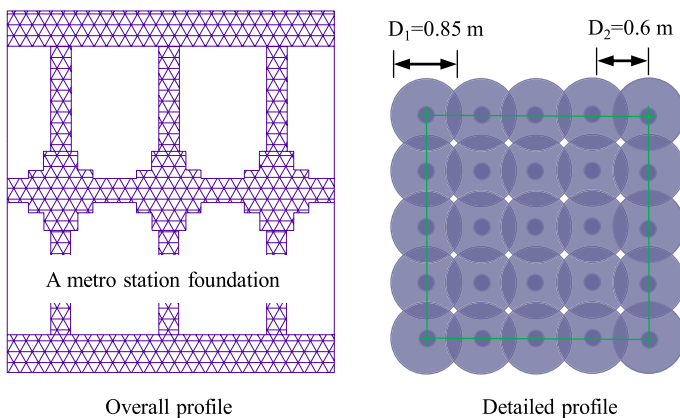


Fig. 12 Basement reinforcement by jet-grouting pile in metro station. *Note:* D_1 is pile diameter and D_2 is pile space. After Liu (2018)

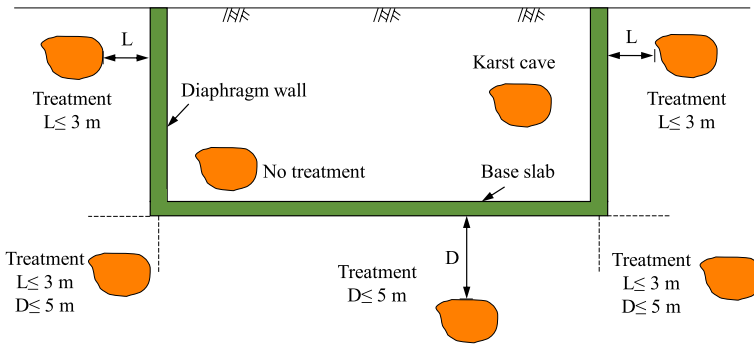


Fig. 13 Illustration of diaphragm wall applied in Wuhan metro system (created based on the concept of Liu 2018)

For the case of metro constructed in downtown areas or crowded regions, He et al. (2017) developed the grouting curtain technique for cutting off water flow, it not only ensures metro system safety, but also addresses the issues of large construction site during waterproofing structure installation. It can be seen from Fig. 14 that this technique was commonly composed of the upper bored or jet-grouting pile and the lower grouting curtain. It minimizes adverse impacts of the karst caves on metro tunnels from two aspects, that is, load-bearing capacity improvement and water flow isolation.

5.5 Shield machine parameter optimization

In addition to above-mentioned treatment measures and safe construction guidelines, there are other benefits to be derived from optimization of shield machines and their accessory elements (Qu and Zhou 2016). These can be summed up as:

1. In terms of the shield segment designed for avoiding uneven settlement of tunnel structures and ensuring a safe construction, the following considerations should be taken into account: (a) adopting reinforced concrete segment, (b) adopting high strength bolt, (c) setting rebate at longitudinal joints of segment to increase longitudinal stiffness, and (d)

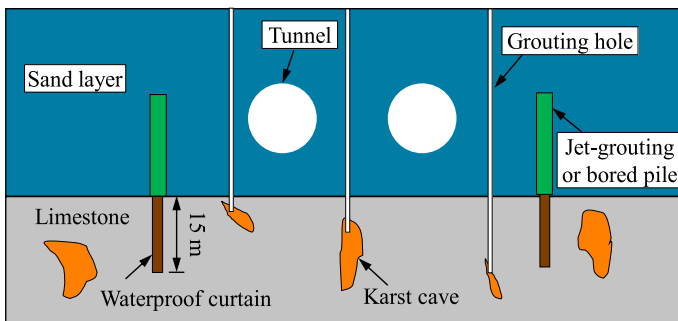


Fig. 14 Illustration of a grouting curtain for cutting off water (after He et al. 2017)

adding reserved grouting hole to ensure the conditions of reinforcement on the stratum after the metro is put into operation.

- Control the driving parameters of shield. (a) when water pressure is too large, the pressure pump device should be in operation to reduce construction disturbance on surrounding ground, and (b) synchronous grouting should be sufficient and secondary grouting should block groundwater passage timely, and thus stabilize shield segments.

6 Case history

The first-stage project of the Wuhan metro line 6 starts from Dongfeng Company station and ends at the Jinyinhu Park station, and it has 27 underground stations with a total length of 36.1 km. The study section focus is between Qianjincun station and Mayinlu station, which mainly underwent the aforementioned I-type and II-type karst geology structures.

6.1 Description of metro construction site

The project site is dominated by the Grade-I terrace of the Yangtze river, where the bedrock is buried under the Quaternary stratum. The geological structures are mainly folding and fault, while fracture structures are found through the drilling cores. The site is located in the Tangjiashan-Xinancun fan-shaped syncline, and the core of the syncline is dominated by the Guanyinshan formation of Triassic, and two limbs are dominated by the Daye formation of the Triassic and Wutong formation of the Devonian. One fault (labelled F1) was detected at the site, and it is mainly filled with argillaceous limestone with strong crush and corrosion (Fig. 15). The groundwater in the project site is mainly the upstream water, with some pore confined water and bedrock fissure water, as shown in Table 4.

6.2 Countermeasures applied in Wuhan metro line 6

To avoid occurrence of hazards during metro tunnel construction, a series of countermeasures were adopted during the construction stage of the Wuhan metro line 6. The main purpose is to, (a) cut-off water leakage path between overlying layer and karst caves; (b) reinforce overlying loose layers, especially the fine sand layer, and prevent seepage-type sand-carrying action caused by karst collapse from affecting the stability of shield segment

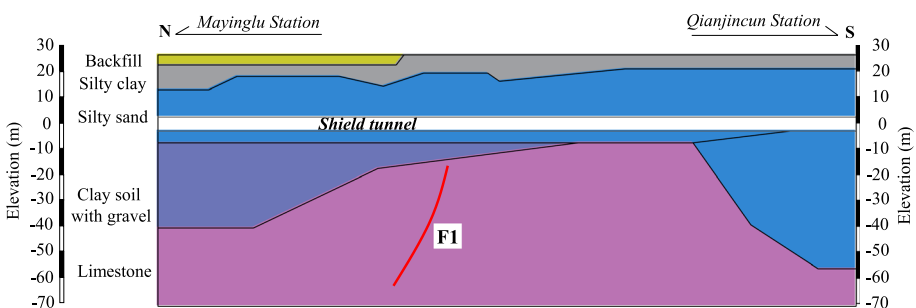


Fig. 15 Sectional view of geologic conditions of the case project. After Gao (2017) and He et al. (2017)

Table 4 Hydrogeology conditions of the case project. Data from Xu et al. (2017)

No.	Type	Depth (m)	Description
1	Upstream water	18.8–21.5	Mainly distributed in the upper backfill layer, supplemented by atmosphere rainfall
2	Pore confined water	15.5–17.6	Mainly supplemented by lateral seepage of groundwater with sufficient amount, and mainly influenced by seasonal variation
3	Bedrock fissure water	–	Mainly supplemented by downward seepage of the upper groundwater

structures. The countermeasures used in this case history are summarized as follows (Gao 2017).

1. The full-grouting filling method was employed for shallow karst caves around the metro tunnel based upon drilling surveys. By eliminating hidden danger of slurry exudation, it guaranteed a better effectiveness of the grouting and was verified by conducting regular field measurements, in which the maximum value of the ground heave was 2.26 mm throughout the grouting period (Fig. 16a).
2. One row or more rows of curtain grouting holes are set in the bedrock surface of the lower limestone. The drilling holes are of 10 m below the bedrock surface, with a plum-blossom-shape arrangement, and thus forming a vertical isolated diaphragm wall. The in situ observations revealed a great filling effect of the caves inside the wall, and no cases of less or excessive grouting were observed (Fig. 16b).
3. A full-range of grouting was employed to improve the strength of the interface between soil and rock below the shield tunnel. To ensure its reliability, some detailed techniques and requirements need to be considered: (a) the drilling-hole deviation from designed position is less than 10 cm; (b) an automatic grouting recorder should be used to control the grouting pressure in a range of 0.3–0.5 MPa. (c) at the maximum grouting pressure of 0.5 MPa, the grouting rate is less than 1 L/min (Fig. 16c).
4. In some cases such as difficulties and poor effectiveness of grouting encountered in sand layers above the karst, jet-grouting pile reinforcement was used for treatment. The 80-cm-diameter piles were arranged in a space of 60 cm and the length embedded in the bedrock is not less than 50 cm.

6.3 Feedback analysis of monitoring data

To avoid large deformation and failure of shield segment caused by cave collapse, its displacement value must be strictly controlled during tunnel construction to prevent ground



Fig. 16 Photographs of in situ slurry grouting. **a**, **b** and **c** are sealed grouting hole, cement slurry solid and drill core after grouting (Gao 2017)

collapse. Gao (2017) conducted a series of in situ measurements and studied treatment effectiveness from the monitoring data. Table 5 presents a brief introduction to karst caves in this case history. After implementing the treatment measures, vertical deformation and horizontal convergence of segment structures were monitored regularly, and the results are plotted in Fig. 17.

The results indicate that the vault settlement, bottom uplift and horizontal convergence increase linearly within 30 d, and then tend to grow slowly, and finally tend to be stable. The vault settlement, bottom uplift and horizontal convergence at the sections of K11 + 804 and K11 + 877 are -4.34 mm, 2.05 mm, 8.82 mm and -6.2 mm, 4.83 mm and 10.26 mm, respectively. The effectiveness of the proposed countermeasures is verified by small deformation amount and reduction in the time needed to achieve stability.

7 Conclusions

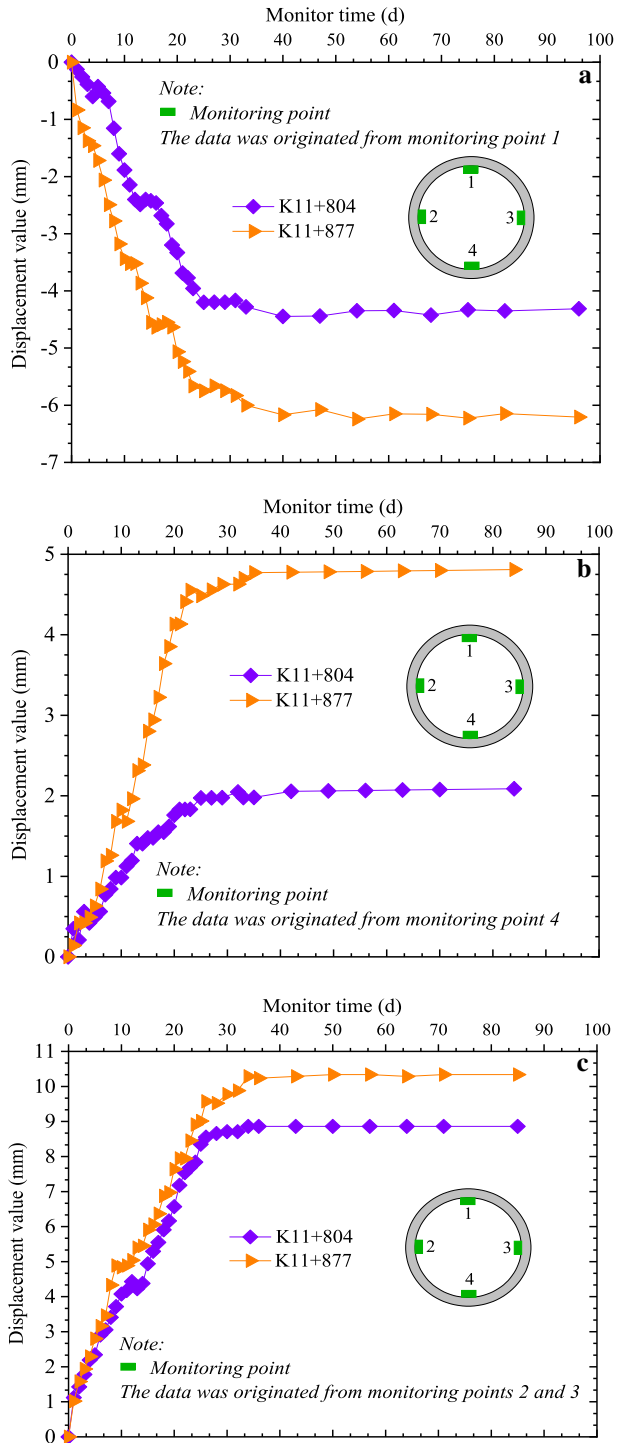
The geology and karst conditions in Wuhan are studied, and a series of countermeasures were summarized for hazards and risk mitigation during metro system construction in this paper, and the following conclusions can be drawn:

1. Wuhan is characterized by unique, but complex geological conditions, and developed a large area of the karst geology. The twice transgression-regression cycles during the late Palaeozoic and the early Mesozoic eras, forming two sets of carbonate strata of the Huanglong formation of the middle Carboniferous and the Daye and Guanyinshan formations of the lower Triassic, which provide the material basis for karst development.
2. Under the influence of the tectonic action, the underlying bedrock in Wuhan distributes in an approximate east to west direction. There are six karst belts that have been detected in the main urban area of Wuhan, and five types of karst geological structure were obtained based on the differences of geological performance of the overlying rock-soil layers.
3. Due to the wide distribution of karst geology in Wuhan, a shield tunnel constructed in karst region may disrupt its stable state, and then results in a host of engineering problems and hazards, such as (a) water ingress and mud inrush, (b) partial karst ground collapse, (c) damage and failure of shield machine, and (d) metro operation and management issues.
4. To eliminate tunnelling-induced geo-hazards, several countermeasures were summarized, which includes (a) karst cave detection and early warning system, (b) slurry grouting techniques, (c) ground improvement, (d) waterproofing techniques, and (e) shield machine parameter optimization. These suggested countermeasures can be flexibly applied as the geological conditions vary to ensure safe construction and operation of the metro tunnel in karst region.

Table 5 Description for karst caves in case history. Data from Gao (2017)

Section	Cave size		Cave roof thickness (m)	Distance between tunnel and bedrock (m)
	Height (m)	Span (m)		
K11 + 804	2.78	3.17	0.41	15.3
K11 + 877	3.5	2.79	0.6	14.8

Fig. 17 In situ monitoring data. **a**, **b** and **c** are vault settlement, bottom uplift and horizontal convergence. Data from Gao (2017)



5. The case history regarding the Wuhan metro line 6, in which the tunnel passing through the typical karst stratum, was referred for further analysis. The countermeasures used during tunnel construction include the slurry grouting, ground improvement and waterproof treatment. The measured vault settlement, bottom heave and horizontal convergence at sections of K11 + 804 and K11 + 877 are -4.34 mm, 2.05 mm, 8.82 mm and -6.2 mm, 4.83 mm and 10.26 mm, respectively, verifying the effectiveness of these adopted measures.

Acknowledgements Financial supports from the Fundamental Research Funds for the Central Universities, CHD (No. 300102219711, No. 300102219716, No. 300102219723 and No. 300102210530), the National Natural Science Foundation of China (No. 51978066), the National Key R&D Program of China (No. 2018YFC0808706) and the Project on Social Development of Shaanxi Provincial Science and Technology Department (No. 2018SF-382, No. 2018SF-378) are sincerely acknowledged.

References

- Alija S, Torrijo FJ, Quinta-Ferreira M (2013) Geological engineering problems associated with tunnel construction in karst rock masses: the case of Gavarres tunnel (Spain). *Eng Geol* 157(4):103–111. <https://doi.org/10.1016/j.engeo.2013.02.010>
- Bai L, Jiang LM, Wang HS, Sun QS (2016) Spatiotemporal characterization of land subsidence and uplift (2009–2010) over Wuhan in central china revealed by TerraSAR-X InSAR analysis. *Remote Sens* 8(4):350. <https://doi.org/10.3390/rs8040350>
- Cao LQ, Zhang DL, Fang Q (2020) Movements of ground and existing structures induced by slurry pressure-balance tunnel boring machine (SPB TBM) tunnelling in clay. *Tunn Undergr Space Technol* 97:2020
- Cheng WC, Li G, Liu N, Xu J, Horpibulsuk S (2020) Recent massive incidents for subway construction in soft alluvial deposits of Taiwan: a review. *Tunn Undergr Space Technol* 96:103178. <https://doi.org/10.1016/j.tust.2019.103178>
- Cui QL, Wu HN, Shen SL, Xu YS, Ye GL (2015) Chinese karst geology and measures to prevent geohazards during shield tunnelling in karst region with caves. *Nat Hazards* 77(1):129–152. <https://doi.org/10.1007/s11069-014-1585-6>
- Ding LY, Wu XG, Li H, Luo HB, Zhou Y (2011) Study on safety control for Wuhan metro construction in complex environments. *Int J Project Manag* 29(7):797–807. <https://doi.org/10.1016/j.ijproman.2011.04.006>
- Fan SK (2006) A discussion on karst collapse in Wuhan (Hubei). *Resources Environment and Engineering* 20:608–616 (**in Chinese**)
- Gao SM (2017) Research on force characteristic of subway shield tunnel's structure in underlying karst stratum. Ph.D. thesis. Faculty of Engineering, China University of Geosciences, Wuhan, China (**in Chinese**)
- Gui H, Song X, Lin M (2017) Water-inrush mechanism research mining above karst confined aquifer and applications in North China coalmines. *Arab J Geosci* 10(7):1–9. <https://doi.org/10.1007/s12517-017-2965-5>
- He B, Zhong SH, Luo QQ, Zhan BH, Chen C (2017) Characteristics of karst development and karst treatments of Wuhan metro line 6. *Sci Technol Eng* 17(30):336–342 (**in Chinese**)
- Huang QH, Cai YL (2007) Spatial pattern of karst rock desertification in the middle of Guizhou Province, Southwestern China. *Environ Geol* 52(7):1325–1330. <https://doi.org/10.1007/s00254-006-0572-y>
- Huang F, Zhao LH, Ling TH, Yang XL (2017) Rock mass collapse mechanism of concealed karst cave beneath deep tunnel. *Int J Rock Mech Min Sci* 91:133–138. <https://doi.org/10.1016/j.ijrmm.2016.11.017>
- Knez M, Slabe T, Šebela S, Gabrovšek F (2008) The largest karst cave discovered in a tunnel during motorway construction in Slovenia's Classical Karst (Kras). *Environ Geol* 54(4):711–718. <https://doi.org/10.1007/s00254-007-0840-5>
- Li SK, Tao L (2015) Features of karst development in Wuhan area and treatment of karsts encountered in construction of Wuhan metro. *Tunn Constr* 35(5):449–454 (**in Chinese**)

- Li SC, Zhou ZQ, Ye ZH, Li LP, Zhang QQ, Xu ZH (2015) Comprehensive geophysical prediction and treatment measures of karst caves in deep buried tunnel. *J Appl Geophys* 116:247–257. <https://doi.org/10.1016/j.jappgeo.2015.03.019>
- Li P, Wang F, Fang Q (2018) Undrained analysis of ground reaction curves for deep tunnels in saturated ground considering the effect of ground reinforcement. *Tunn Undergr Space Technol* 71:579–590. <https://doi.org/10.1016/j.tust.2017.11.001>
- Liu JF (2018) The karst development characteristics and karst treatment measures of Wuhan Metro line 6. *Urban Geotech Investig Surv* 3:160–165 (in Chinese)
- Liu T, Xie Y, Feng ZH, Luo YB, Wang K, Xu W (2020a) Better Understanding the Failure Modes of Tunnels Excavated in the Boulder-Cobble Mixed Strata by Distinct Element Method. *Eng Fail Anal* 118:104599
- Liu T, Zhong YJ, Han ZL, Xu W (2020b) Deformation characteristics and countermeasures for a tunnel in difficult geological environment in NW China. *Adv Civ Eng* 2020:1694821
- Luo XJ (2013) Features of the shallow karst development and control of karst collapse in Wuhan. *Carsol Sin* 32(4):419–432 (in Chinese)
- Ma EL, Lai JX, Wang LX, Xu SS, Li CJ, Guo CX (2020) Cutting-edge Sensing Technologies for Urban Underground Construction. *Measurement* 165:107857
- Maeda M, Kushiyama K (2005) Use of compact shield tunneling method in urban underground construction. *Tunn Undergr Space Technol* 20(2):159–166. <https://doi.org/10.1016/j.tust.2003.11.008>
- Ning GM, Chen GJ, Xu SY, Xiao Y (2006) Engineering geological research on the underground space of Wuhan city. *Hydrogeol Eng Geol* 33(6):29–35 (in Chinese)
- Qin YW, Lai JX, Qiu JL, Liu T (2020) Arching Effect and Collapse Evolution Law of Tunnel in Boulder-Cobble Mixed Formation. *Tunn Undergr Sp Technol* 107:107403
- Qiu JL, Lu YQ, Lai JX, Zhang YW, Yang T, Wang K (2020a) Experimental study on the effect of water gushing on loess metro tunnel. *Environ Earth Sci* 79(11):1–12. <https://doi.org/10.1007/s12665-020-08995-4>
- Qiu JL, Lu YQ, Lai JX, Guo CX, Ke Wang (2020b) Failure behavior investigation of loess metro tunnel under local-high-pressure water environment. *Eng Fail Anal* 112(4):125–138
- Qu RF (2017) Research on the evolutive process of karst collapse and the impact mechanism of the karst on Subway tunnel in Wuhan Subway crossing area. Ph.D. thesis, Faculty of Engineering, China University of Geosciences, Wuhan, China. (in Chinese)
- Qu RF, Zhou CB (2016) On the influence of karst collapse on subway tunnel and karst treatment in Wuhan. *Electron J Geotech Eng* 21(10):3979–3992
- Ren DJ, Shen SL, Cheng WC, Zhang N, Wang ZF (2016) Geological formation and geo-hazards during subway construction in Guangzhou. *Environ Earth Sci* 75(11):1–14. <https://doi.org/10.1007/s12665-016-5710-6>
- Song ZP, Shi GL, Zhao BY, Zhao KM, Wang JB (2020) Study of the stability of tunnel construction based on double-heading advance construction method. *Adv Mech Eng* 12(1):1–17
- Sun SQ, Li LP, Wang J, Shi SS, Song SG, Fang ZD, Ba XZ, Jin H (2018) Karst development mechanism and characteristics based on comprehensive exploration along Jinan metro, China. *Sustainability* 10:3383. <https://doi.org/10.3390/su10103383>
- TROWM (2014) Technical part of the report on karst treatment of the Wuhan Metro Line 27. Wuhan Metro Group Co., Ltd, Wuhan (in Chinese)
- Waltham AC, Fookes PG (2003) Engineering classification of karst ground conditions. *Q J Eng Geol Hydrogeol* 36(5):101–118. <https://doi.org/10.1144/1470-9236/2002-33>
- Wang L (2014) Tunnel in karst stratum of city disaster prevention technology of subway. MS thesis, School of Civil Engineering, Shijiazhuang Tiedao University, Shijiazhuang, China (in Chinese)
- Wang SJ, Liu QM, Zhang DF (2004) Karst rocky desertification in Southwestern China: geomorphology, landuse, impact and rehabilitation. *Land Degrad Dev* 15(2):115–121. <https://doi.org/10.1002/ldr.592>
- Wang YC, Yin X, Jing HW, Liu RC, Su HJ (2016a) A novel cloud model for risk analysis of water inrush in karst tunnels. *Environ Earth Sci* 75(22):1450. <https://doi.org/10.1007/s12665-016-6260-7>
- Wang YC, Jing HW, Yu LY, Su HJ, Luo N (2016b) Set pair analysis for risk assessment of water inrush in karst tunnels. *Bull Eng Geol Environ* 2016:1–9. <https://doi.org/10.1007/s10064-016-0918-y>
- Wang YQ, Wang ZF, Cheng WC (2018a) A review on land subsidence caused by groundwater withdrawal in Xi'an, China. *Bull Eng Geol Environ* 4:1–13. <https://doi.org/10.1007/s10064-018-1278-6>
- Wang ZF, Cheng WC, Wang YQ (2018b) Investigation into geohazards during urbanization process of Xi'an, China. *Nat Hazards* 92(3):1937–1953. <https://doi.org/10.1007/s11069-018-3280-5>
- Wang W, Gao SM, Liu LF, Wen WS, Li P, Chen JP (2018c) Analysis on the safe distance between shield tunnel through sand stratum and underlying karst cave. *Geosyst Eng* 22(2):81–90. <https://doi.org/10.1080/12269328.2018.1475265>

- Wang XL, Lai JX, Qiu JL, Xu W, Wang LX, Luo YB (2020a) Geohazards, reflection and challenges in Mountain tunnel construction of China: a data collection from 2002 to 2018. *Geomat Nat Hazards Risk* 11(1):766–784. <https://doi.org/10.1080/19475705.2020.1747554>
- Wang LX, Xu SS, Qiu JL, Wang K, Ma EL, Li CH, Guo CX (2020b) Automatic monitoring system in underground engineering construction: review and prospect. *Adv Civ Eng*. <https://doi.org/10.1155/2020/3697253>
- Wang ZF, Shen SL, Modoni G, Zhou AN (2020c) Excess pore water pressure caused by the installation of jet grouting columns in clay. *Comput Geotech* 125:103667
- Wang LX, Ma EL, Li H, Lai JX, Xu SS, Wang K, Liu T (2020d) Tunnelling Induced Settlement and Treatment Techniques for a Loess Metro in Xi'an. *Adv Civ Eng* 2020:1854813
- Wei Y, Sun S (2017) Study on formation and expansion condition of hidden soil cavity under condition of groundwater exploitation in karst areas. *Environ Earth Sci* 76(7):282. <https://doi.org/10.1007/s12665-017-6601-1>
- WGSC (2018) Wuhan Geological Survey Center, <http://www.whgcs.cn/>. (in Chinese)
- WHRT (2018) Wuhan Metro Group Co., Ltd. <http://www.whrt.gov.cn/>. (in Chinese)
- Wu H, Zhong YJ, Xu W, Shi W, Shi XH (2020a) Experimental investigation of ground and air temperature fields of a cold-region road tunnel in NW China. *Adv Civi Eng*. Article ID 4732490, 12 pages. <https://doi.org/10.1155/4732490>
- Wu H, Yao CK, Li CH, Miao M, Zhong YJ, Lu YQ, Liu T (2020b) Review of application and innovation of geotextiles in geotechnical engineering. *Materials* 13:1–16. <https://doi.org/10.3390/ma13071774>
- Wu K, Shao ZS, Li CL, Qin S (2020c) Theoretical Investigation to the effect of bolt reinforcement on tunnel viscoelastic behavior. *Arab J Sci Eng* 45(6):152–163. <https://doi.org/10.1007/s13369-019-04215-9>
- Xu HQ, Chen L, Zhou SD, Luo QQ, Xu JB, He B (2017) Collapse mechanism and treatment technology of the karst regions in city metro. *Sci Technol Eng* 17(8):282–287 (in Chinese)
- Yang XL, Xiao HB (2016) Safety thickness analysis of tunnel floor in karst region based on catastrophe theory. *J Central South Univ* 23(9):2364–2372. <https://doi.org/10.1007/s11771-016-3295-6>
- Zhang ZQ, Zhang KJ, Dong WJ, Zhang B (2020a) Study of rock-cutting process by disc cutters in mixed ground based on three dimensional particle flow model. *Rock Mech Rock Eng* 53(6):122–139. <https://doi.org/10.1007/s00603-020-02118-y>
- Zhang ZQ, Sun F, Chen BK (2020b) Thermal-mechanical coupled analysis for tunnel lining with circular openings. *Tunn Undergr Space Technol* 97:103409. <https://doi.org/10.1016/j.tust.2020.103409>
- Zhang CP, Li W, Zhu WJ, Tan ZB (2020c) Face stability analysis of a shallow horseshoe-shaped shield tunnel in clay with a linearly increasing shear strength with depth. *Tunn Undergr Space Technol* 97:578–591. <https://doi.org/10.1016/j.tust.2020.103291>
- Zhou L, Guo JM, Hu JY, Li JW, Xu YF, Pan YJ, Shi M (2017) Wuhan surface subsidence analysis in 2015–2016 based on Sentinel-1A data by SBAS-InSAR. *Remote Sens* 9(10):982. <https://doi.org/10.3390/rs9100982>
- Zini L, Chiara C, Franco C (2015) The challenge of tunneling through Mediterranean karst aquifers: the case study of Trieste (Italy). *Environ Earth Sci* 74(1):281–295. <https://doi.org/10.1007/s12665-015-4165-5>

Publisher's Note Springer Nature remains neutral with regard to jurisdictional claims in published maps and institutional affiliations.